I J C T A, 9(5), 2016, pp. 2467-2481
© International Science Press

Computation of Supersonic Cold Cavity Flow

Dinesh M.*, Anish Alfred Joe and Mohammed Cassim Sannan*****

ABSTRACT

A commercial CFD code, FLUENT has been used to compute cavity flow. Geometric modeling and grid generation is carried out by using GAMBIT pre-processor. Simulation has been carried out using FLUENT. The 2-D steady state Reynolds Averaged Navier-stokes (RANS) along with RNG k-e turbulence model has been solved for cavity flow. The convective terms have been discretized by second order upwind scheme for all the equations. However, diffusive terms have been discretized by central differencing. The SIMPLE algorithm of pressure based method is used to compute the flow. The algebraic equations are solved in segregated manner. The algebraic multi grid (AMG) has been used to accelerate the convergence. The equations have been solved iteratively by Gauss Siedel method. The converged solution predicted the basic flow features like recirculation of flow inside the cavity, free shear layer over the cavity, reattachment of flow on the slanted wall followed by the recompression, adverse pressure gradient on the slanted wall etc. very well. The predicted result is compared with the experimental results and is agreed well with the experiment qualitatively.

Keywords: CFD, Flow in cavity, Reattachment of flow, free shear layer.

1. INTRODUCTION

1.1. Cavity

The term cavity in SCRAMJET generally refers as passive device to achieve two different properties. One of them is to improve mixing of fuel and air and the other is to hold the flame in SupersonicCombustion Ram-jet (SCRAMJET).These two different properties can be achieved at different aspect (L/D) ratio of the Cavity. In general, the boundary layer ahead of the cavityseparates at the leading edge and forms a free shear layer across the cavity. Inside the cavity, flow recirculation takes place. The shear layer reattaches at some other point downstream. The reattachment point depends upon the geometry of the cavity and the external flow conditions. Depending upon the reattachment point, the cavities are classified as" open" or "closed". In open cavity, the reattachment takes place at the rear wall of the cavity and in closed cavity it takes place on the lower wall. The open cavities have aspect ratio less than about 7-10 while the closed cavities have higher aspect ratios. Depending upon the pressure inside the cavity, the separated free shear layer may be locally detected upwards or downwards producing a shock wave or an expansion wave at the leading edge. The leading edge expansion wave, flow separation, flow recirculation, reattachment of free shear layer and trailing edge shock contribute to the pressure loss in the cavity which needs to be kept low for acceptable performance.

1.1.1. Classification of cavity

In a broader context, the cavity is classified as "open" or "closed" if the reattachment takes place at the back face of the cavity, the cavity is called "open" cavity but if it takes place on the lower wall, the cavity

* Assistant Professor, Dept. of Aeronautical Engineering, St. Peter's University, Avadi, Chennai-54, *Email: dineshsaviour@gmail.com*

** Final Year, M.E., Dept. of Aeronautical Engineering, St. Peter's University, Avadi, Chennai-54, *Email: anish27joe@gmail.com*

*** Final Year, B.E., Dept. of Aeronautical Engineering, St. Peter's University, Avadi, Chennai-54, *Email: cassimsannan@gmail.com*

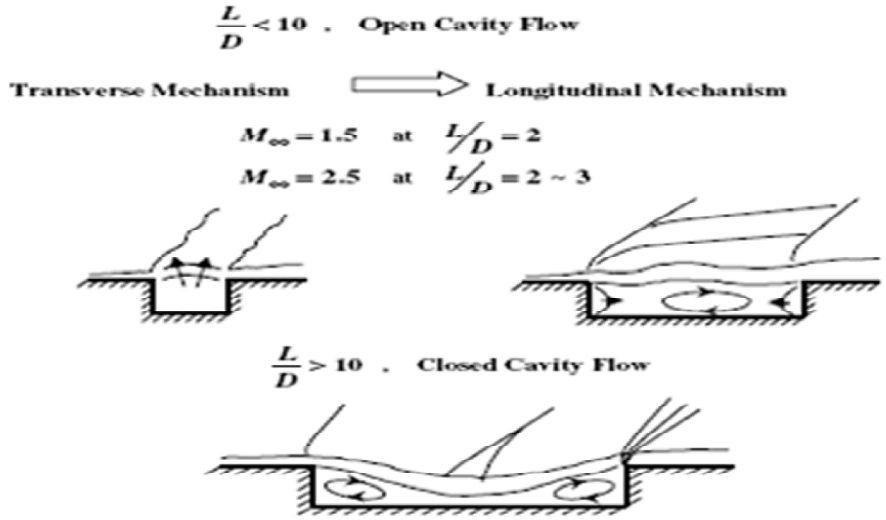

Figure 1: Types of cavity

is called "closed" cavity. The open cavities have aspect ratio less than about 7-10 while the closed cavities have higher aspect ratios. In Open cavity having aspect ratio less than 3, transverse oscillation takes place over the shear layer, while for higher aspect ratio; longitudinal oscillation takes place.

Fig. 1. shows different types of cavities.

1.1.2. Cavities as flame holder

To get the flame holding properties, a recirculation zone inside the cavity with hot pool of radicals must be created which will provide continuous source of ignition thereby reduce the induction time. Generally closed cavity induction time. Generally closed cavity as a flame holder. Cavities having smaller aspect ratio can also be used with proper active or passive self-sustained oscillations control system such as fluid injection at the leading edge, vortex generator, spoiler, slanted trailing edge cavity etc. Cavity can be used as a flame holder in low speed flow as well as high speed flow.

1.1.3. Cavities as a supersonic mixing device

Many researchers observed that the growth rate of mixing layer between air and fuel in scramjet combustor decreases as the convective Mach number increases due to compressibility effects. So cavity with self-sustained oscillation can be used to enhance mixing in free shear layer. The convective Mach number is defined as Mach number of a frame of reference traveling with the large-scale structures of shear layer.

1.2. CFD

Computational Fluid Dynamics (CFD) is the *art* of replacing the differential equation governing the Fluid Flow, with a set of algebraic equations (the process is called discretization), which in turn can be solved with the aid of a digital computer to get an *approximate* solution. The advent of high-speed and large-memory computers has enabled CFD to obtain solutions to many flow problems including those that are compressible or incompressible, laminar or turbulent, chemically reacting or non-reacting. The well-known discretization methods used in CFD are Finite Difference Method (FDM), Finite Volume Method (FVM), Finite Element Method (FEM), and Boundary Element Method (BEM).

Computational Fluid Dynamics (CFD) has grown from a mathematical curiosity to become an essential tool in almost every branch of fluid dynamics, from aerospace propulsion to weather prediction. As a developing science, Computational Fluid Dynamics has received extensive attention throughout the

international community since the advent of the digital computer. Firstly, the desire to be able to model physical fluid phenomena that cannot be easily simulated or measured with a physical experiment, for example weather systems or hypersonic aerospace vehicles. Secondly, the desire to be able to investigate physical fluid systems more cost effectively and more rapidly than with experimental procedures. In design and development, CFD programs are now considered to be standard numerical tools, widely utilized within industry.

2. LITERATURE REVIEW

[1] An experimental investigation was conducted to study the two dimensional, compressible, turbulent reattaching free shear layer formed by geometrical separation of a Mach 2.46 flow with a turbulent boundary layer and a Reynolds number of 5.01×10^7m from a 25.4 mm length high backward-facing step. The wind tunnel test section was specifically designed to obtain a constant pressure separation at the step. A detailed survey of the flow field was made utilizing a schlieren system, static pressure taps, and a two-component coincident laser Doppler velocimeter. In contrast to incompressible reattaching free shear layers, significant increases in the turbulence level, significant increases in the turbulence level, shear stress and turbulent triple products were observed within the reattachment region. Large turbulence structure and enhanced mixing were observed in the redeveloping region.

[8-15] the brief study was done regarding the cavity types and what is the advantage of cavities inhypersonic air vehicle. How we can get the better air fuel mixture and better flame holding qualities.

[4]The various numerical methods are studied for solving the continuity, energy, and mass equations.

3. COMPUTATIONAL DETAILS OF THE PRESENT STUDY

The flow inside the domain has been simulated by solving the Reynolds averaged equations for conservation of mass, momentum, and energy. Finite volume method has been used. The convective terms are discretized by second order upwind schemes for all equations while the diffusive terms are discretized by central differencing schemes. Turbulence in the flow has been modeled using the standard *k*-e turbulence model. In order to render the problem tractable for analysis with limited computational sources and time, the following assumptions are made.

3.1. Assumptions

(i) Flow is steady, compressible and turbulent

(ii) Isothermal flow throughout the domain

(iii) Non-Reacting flow inside the cavity

(iv) Buoyancy effects are negligible

(v) Conjugate heat transfer and radiation effects are neglected

3.2. Geometrical modeling and grid generation

A two-dimensional model of a Slanted Cavity has been modeled using GAMBIT pre-processor.

3.2.1. Procedure followed for modeling geometry

1. Points are created as per the geometry.
2. The edges are created by joining the points and face is formed by using all edges as shown below (Fig. 3).

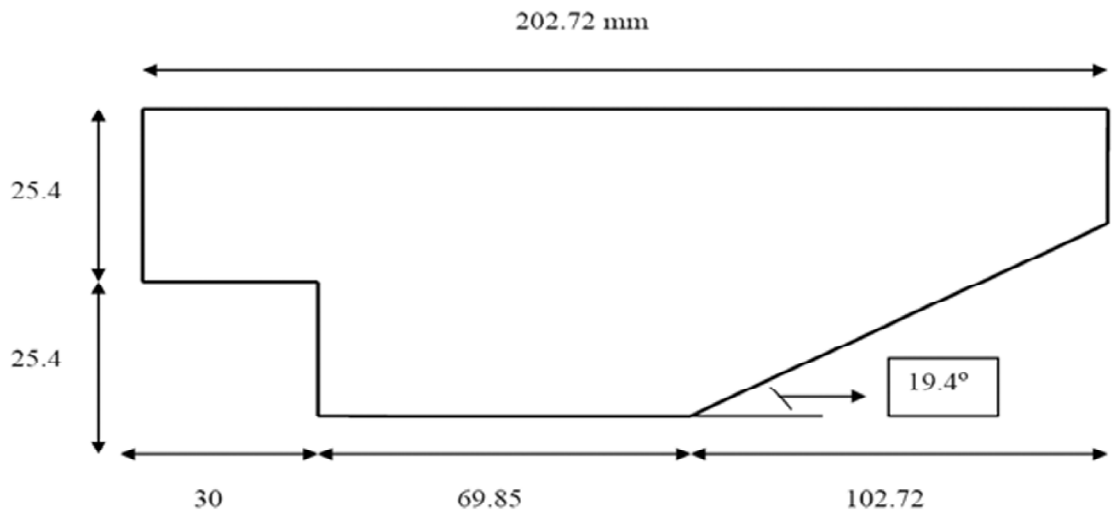

Figure 2: Geometry of the cavity.

Figure 3: A 2-D geometry of the cavity

3.2.2. Grid Generation

1. The geometry is transferred into the meshing section.
2. The boundary layer is created as per boundary layer thickness (Fig 4).
3. The edges are meshed by using the edge mesh tools (Fig 5).
4. The full face of cavity is meshed by using the face mesh tool. (Fig 6).
5. Boundary zones are specified as shown in Fig 7

   The two different grid size domains are considered. And shown below

   The size of the Grid

For grid-1:	**Cells**	**Faces**	**Nodes**	**Partitions**
	22604	45515	22942	1
For grid-2:	**Cells**	**Faces**	**Nodes**	**Partitions**
	32875	66145	33271	1

6. Mesh is exported as .msh file, which is to be read in the solver.

3.3. Salient features

The analysis carried out is presented in the following steps.

- Grid independency is studies for selecting proper interval mesh size.
- Flow behavior is studies inside Cavity.

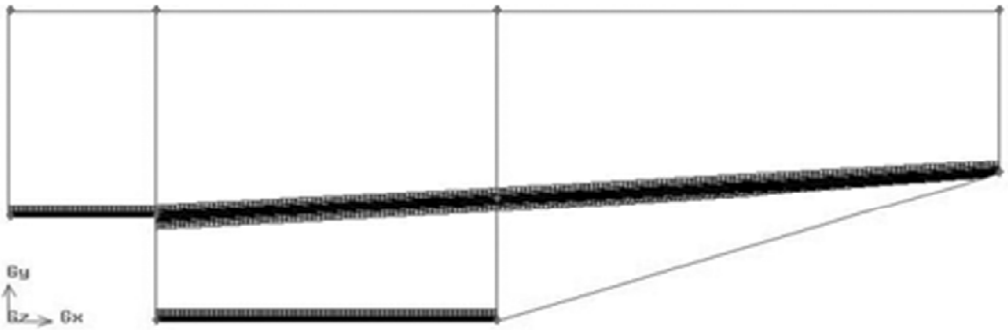

Figure 4: The boundary layer creation

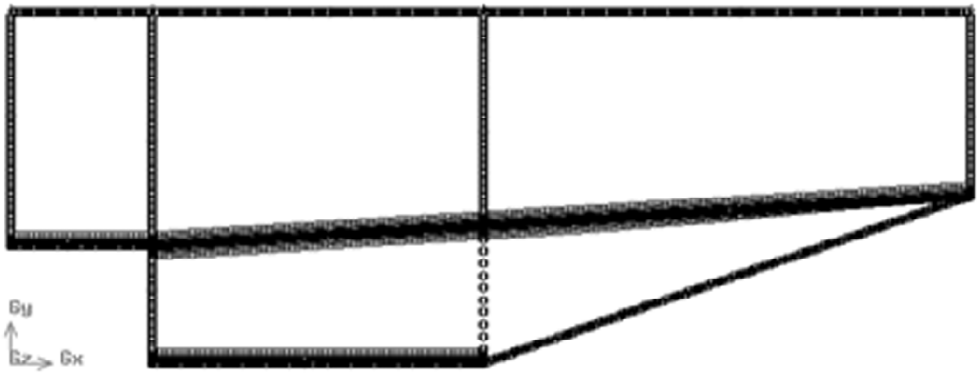

Figure 5: The edge mesh creation

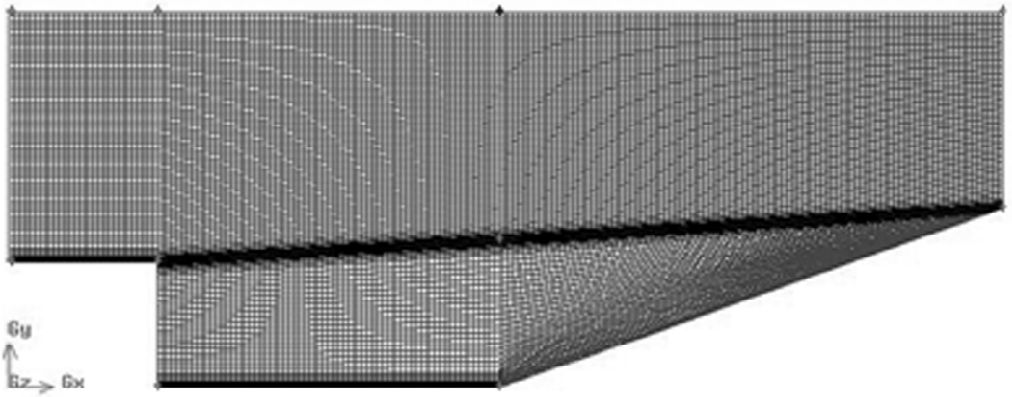

Figure 6: The faces mesh creation

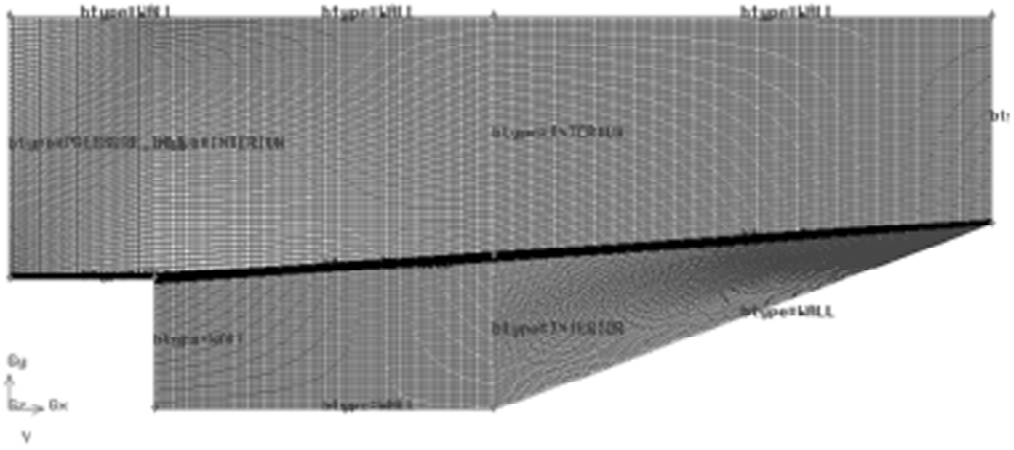

Figure 7: Boundary zones are specified

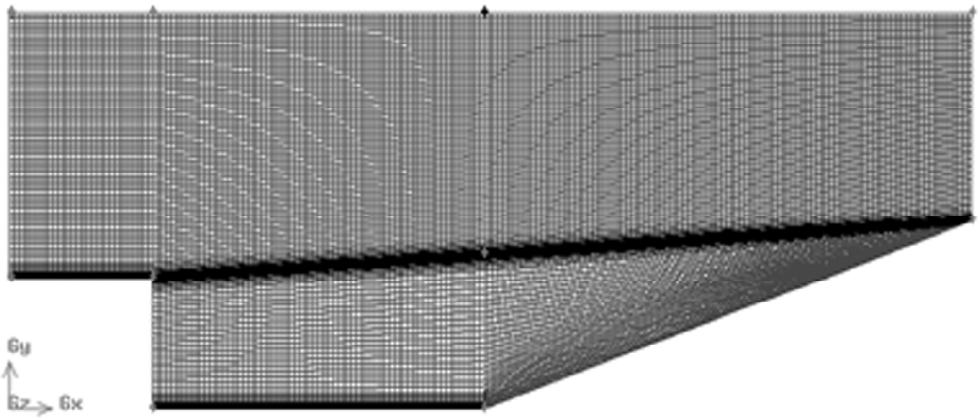

Figure 8: Grid-1

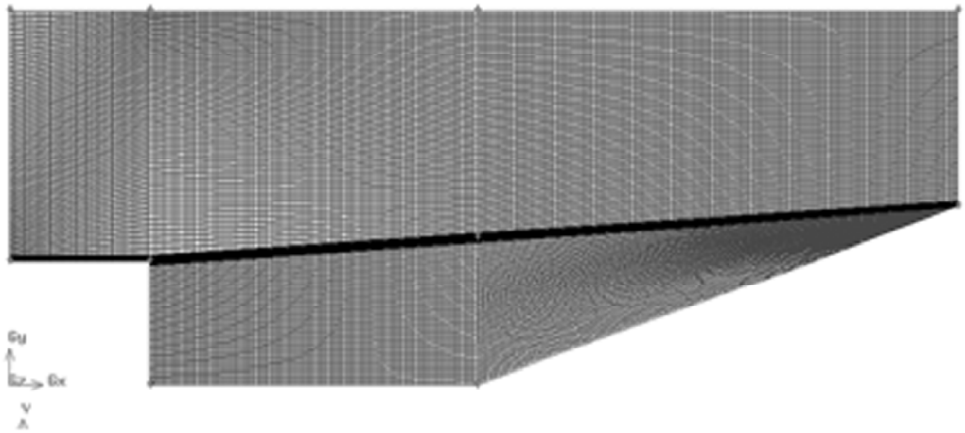

Figure 9: Grid-2

- Analysis is carried out in the Cavity.
- Parametric study is done.

3.3.1. Set up the numerical model

We need to select appropriate conditions for solving a given problem. The conditions like Models, Boundary Conditions, Solver Controls, Relaxation factors, Convergence criterion, Material Properties has to be defined. The solution is get converged in first order upwind scheme. To get better results we go for second order

Models

Model	Settings
Space	2D
Time	Steady
Viscous	RNGk-eturbulence model
Wall Treatment	Standard Wall Functions
Heat Transfer	Disabled
Solidification and Melting	Disabled
Species Transport	Disabled
Coupled Dispersed Phase	Disabled
Pollutants	Disabled
Soot	Disabled

Boundary Conditions Zones

Name	*ID*	*Type*
Medium	1	fluid
Top boundary	3	wall
Slanted Wall	1	Wall
Cavity front wall	1	Wall
Bottom wall	1	Wall
Inlet	1	Pressure-inlet
Outlet	1	pressure-outlet

Operating condition:

X-Component of Flow Direction	1 mm
Y-Component of Flow Direction	25.4 mm

Inlet:

Condition	*Value*
Total Pressure	528100 kpa
Total temperature	297 K
Turb. Kinetic Energy	130.54 m^2/s^2
Turb. Dissipation Rate	107568.6 $m2/s^3$

Outlet:

Since the flow is supersonic, the values of different parameters at outlet will be extrapolated from inside the domain. So there is no need of putting any Boundary Condition at the outlet.

Wall

Condition	*Value*
Enable shell conduction?	No
Wall Motion	0
Shear Boundary Condition	0
Apply a rotational velocity to this wall	No
Velocity Magnitude	0
Wall Roughness Constant	0.5

Solver Controls

Equation	*Solved*
Flow	yes
Turbulence	yes
Energy	yes

Relaxation

Variable	*Relaxation Factor*
Pressure	0.3
Density	1
Body Forces	0.7

(contd...)

(Relaxation contd...)

Variable	*Relaxation Factor*
Momentum	0.4
Turbulence Kinetic Energy	0.5
Turbulence Dissipation Rate	0.5
Turbulent viscosity	1
Energy	0.7

Discretization Scheme

Variable	*Scheme*
Pressure	Standard
Momentum	Second Order Upwind
Density	Second Order Upwind
Turbulence Kinetic Energy	Second Order Upwind
Energy	Second Order Upwind

Convergence criterion

Variable	*check Monitor Convergence*	*Convergence Criterion*
Continuity	yes	0.0001
X-Velocity	yes	0.0001
Y-Velocity	yes	0.0001
Energy	yes	1e-06
K	yes	0.0001
Epsilon	yes	0.0001

Material Properties

		Material: air (fluid)	
Property	*Units*	*Method*	*Value(s)*
Density	kg/m3	ideal Gas	
Cp (Specific Heat)	j/kg-k	constant	1006.43
Thermal Conductivity	w/m-k	constant	0.0242
Viscosity	kg/m-s	Sutherland	

4. RESULTS AND DISCUSSION

Flow inside a cavity has been successfully simulated using the FLUENT commercial code. The present chapter gives a detailed account of the results obtained including the plots of different parameters viz. static pressure, total pressure, velocity magnitude, and Mach number etc.

In the beginning, inlet boundary condition was simulated as uniform values of total pressure and total temperature, but posed in convergence problem. So, by considering this problem as uniform inlet boundary condition, inlet profile boundary has been simulated which converged nicely.

4.1. Total pressure

Fig. 10 and Fig. 11 shows the total pressure contours over the whole computational domain which indicates lower total pressure inside the cavity. As it is well known that the cost of getting flame holding and mixing

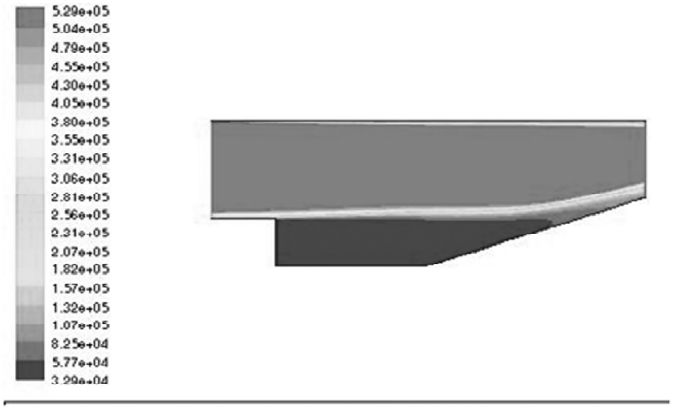

Figure 10: Total pressure contour for grid-1

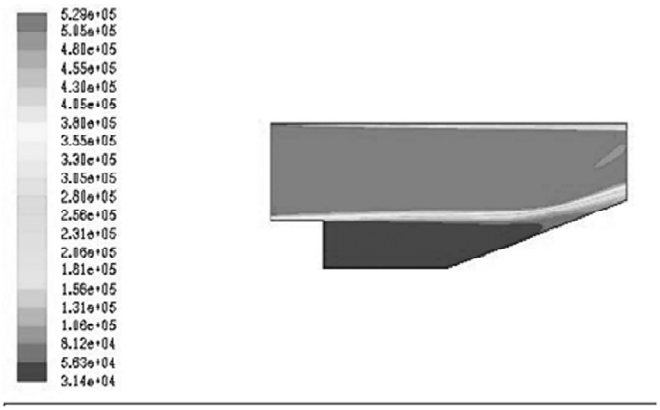

Figure 11: Total pressure contour for grid-2

properties by using cavity is total pressure loss. The total pressures loss is calculated as the ratio of difference of total pressure at the inlet and out let of the domain and inlet total pressure. The values of total pressures are based on mass-weighted average and area-weighted average.

Total pressure loss for grid-1

As per mass-weighted average:

At the inlet mass-weighted average pressure is P_{01} = 517219.3 pa

At out let the mass-weighted average pressure is P_{02} = 482897.2 pa

The total pressure loss = $(P_{01} - P_{02})/ P_{01}$

= (517219.3 - 482897.2) / 517219.3=0.0663

= 6.63%

As per Area-weighted average:

At the inlet area-weighted average pressure is P_{01} = 511038.1 pa

At out let the area-weighted average pressure is P_{02} = 456792 pa

The total pressure loss = $(P_{01} - P_{02})/ P_{01}$

= (511038.1 -456792) /511038.1

= 0.10614 =10.614%

For grid-1 the values of total pressures loss are, based on mass-weighted average is found to be 6.63% and area-weighted average is 10.614%.

Total pressure loss for grid-2

As per mass-weighted average:

At the inlet mass-weighted average pressure is P_{01} = 519259.09 pa

At out let the mass-weighted average pressure is P_{02} = 472897.2 pa

The total pressure loss = $(P_{01} - P_{02})/ P_{01}$

= (519259.09 - 472897.2) / 519259.09 = 0.089284

= 8.9284%

As per Area-weighted average:

At the inlet area-weighted average pressure is P_{01} = 513831.1 pa

At out let the area-weighted average pressure is P_{02} = 456792.3pa

The total pressure loss = $(P_{01} - P_{02})/ P_{01}$

= (513831.1 -456792.3) /513831.1 = 0.11100

= 11.10%

For grid-2 the values of total pressures loss are, based on mass-weighted average is found to be 8.9284% and area-weighted average is 11.10%.

4.2. Static Pressure

The static pressure contour for grid-1 and grid-2 are plotted in fig 12 and 13The adverse pressure gradient, expansion wave, etc can be observed in the figures mentioned above.

4.3. Mach number contour

The Mach number contour for both cases (Fig 14 and Fig 15) is shown below. The free shear layer, recompression zone, oblique shock, etc is clearly visible here. This is well agreeing with the experimental result (Fig 16).

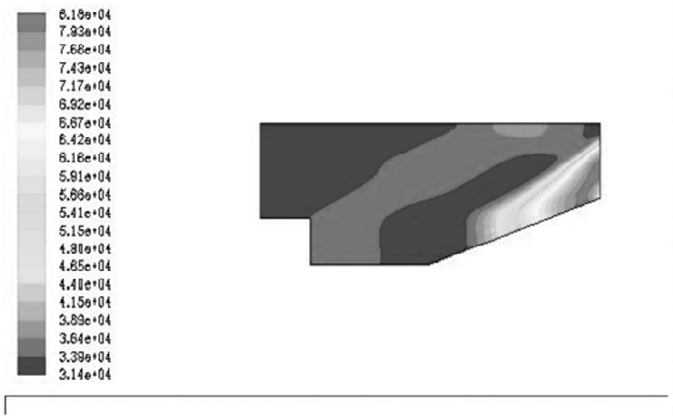

Figure 12: Static pressure contour for grid-1

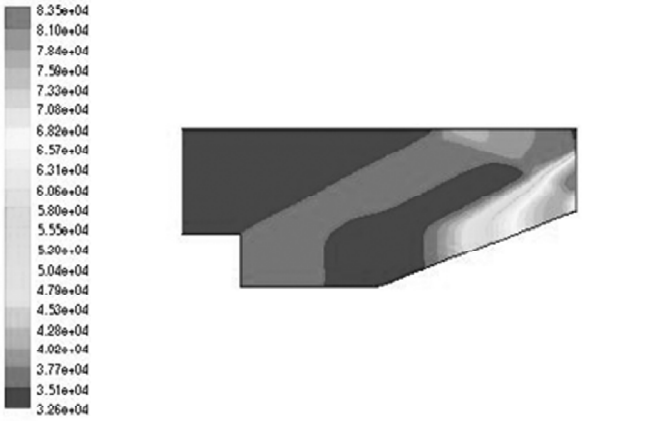

Figure 13: Static pressure contour for grid-2

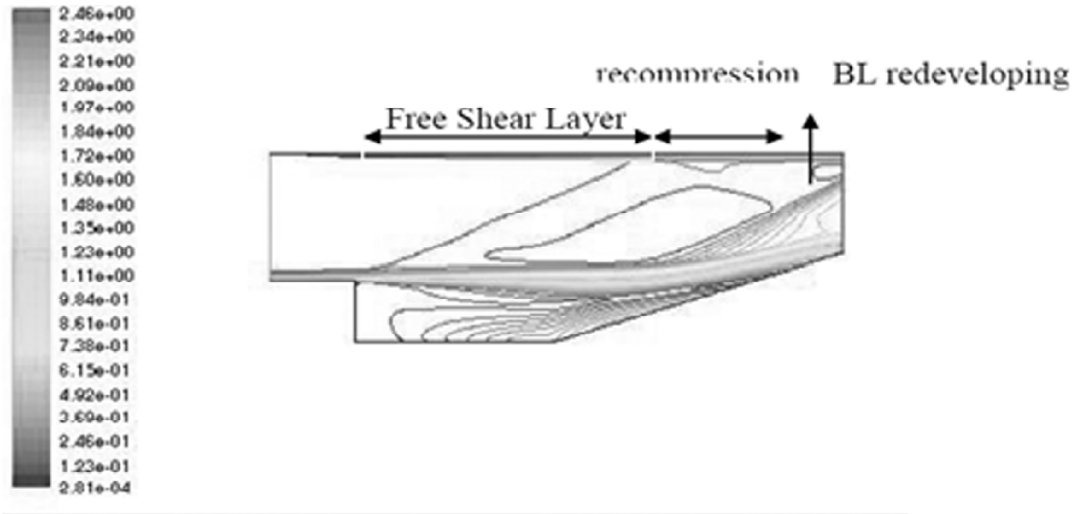

Figure 14: Mach number contour for grid-1

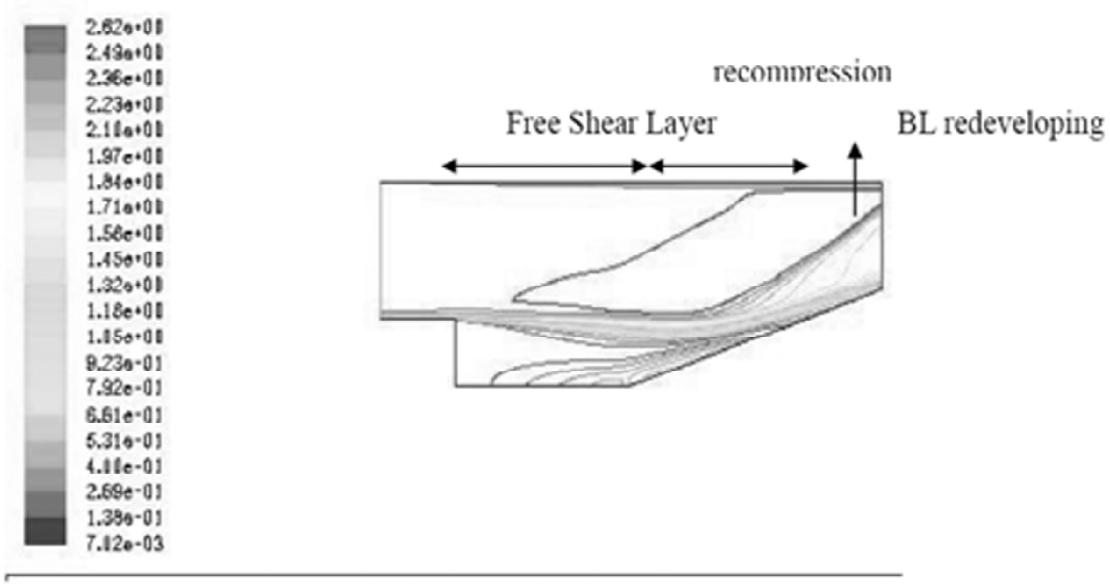

Figure 15: Mach number contour for grid-2

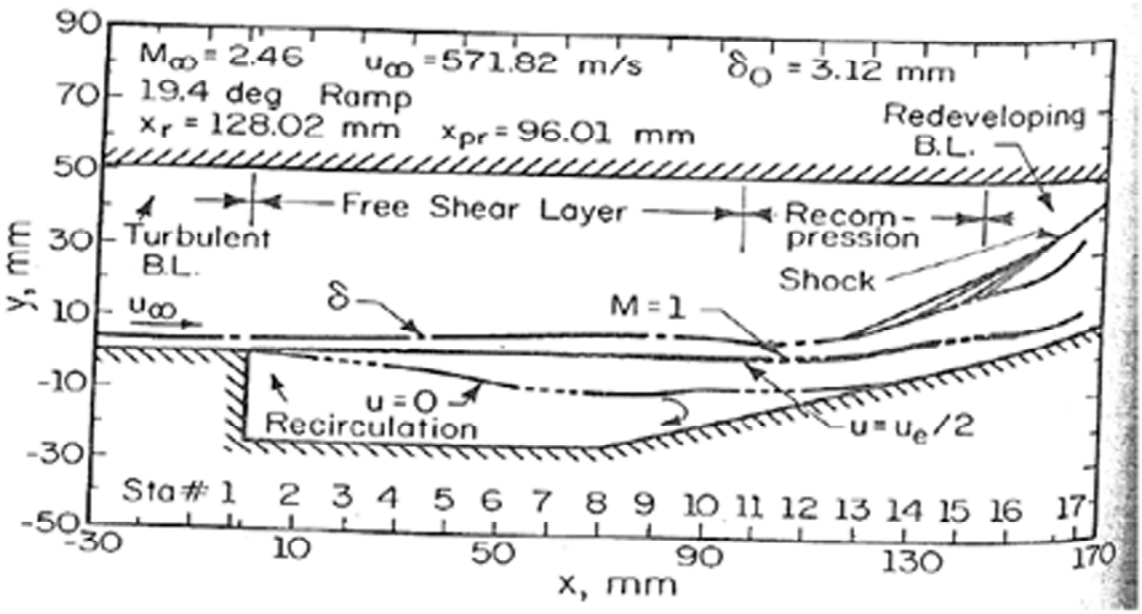

Figure 16: Experimental result (Reference 1)

4.4. Sonic line contour

The sonic line for the grid-1 and grid-2 (Fig 17 and Fig 18) are shown below. Both the predicted sonic lines are qualitatively agreeing well with the experimental result.

4.5. X-direction velocity contour

The X-direction velocity contour for both the grid (Fig 19) and Fig 20) is plotted here. The velocity at the bottom of the cavity is negative in both the cases. This clearly indicates that there must be recirculation of flow inside the cases.

4.6. Velocity vector inside cavity

Recirculation zone is captured for both the cases and compared with the experimental results. The center of recirculation is located at the beginning of slant wall and above the half of the depth of the cavity

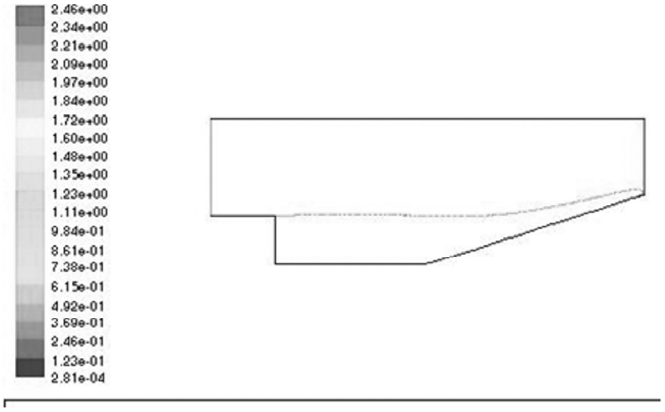

Figure 17: Sonic line contour for grid-1

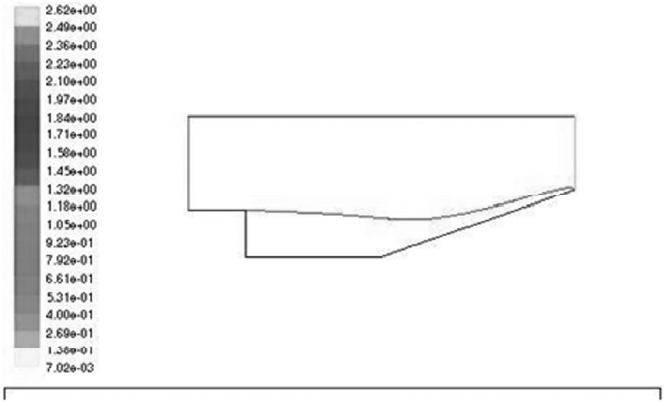

Figure 18: Sonic line contour for grid-2

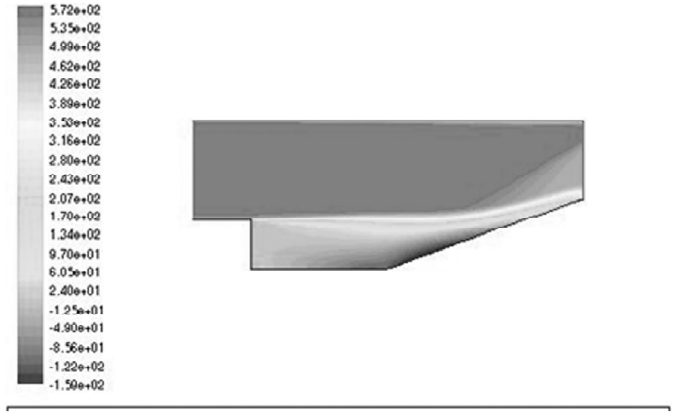

Figure 19: X-direction velocity contour for grid-1

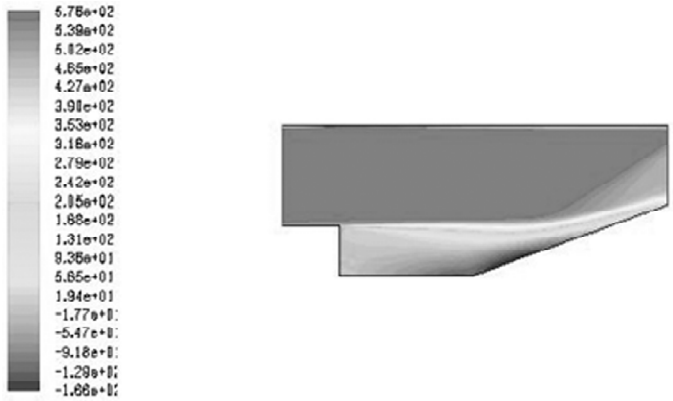

Figure 20: X-direction velocity contour for grid-2

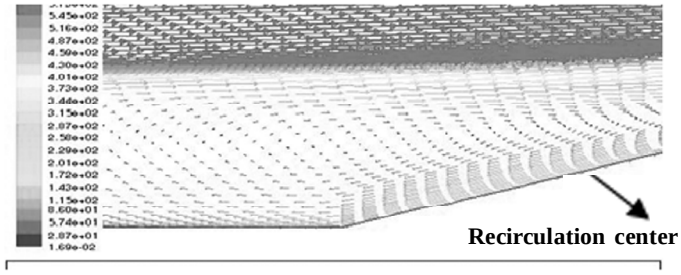

Figure 21: Velocity vector plot for grid-1

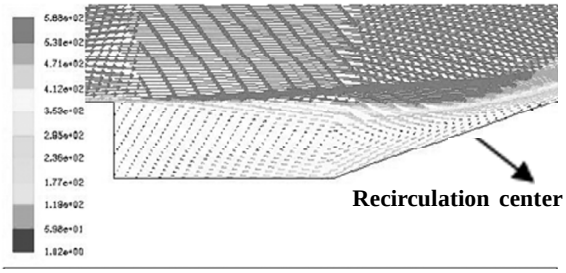

Figure 22: Velocity vector plot for grid-2

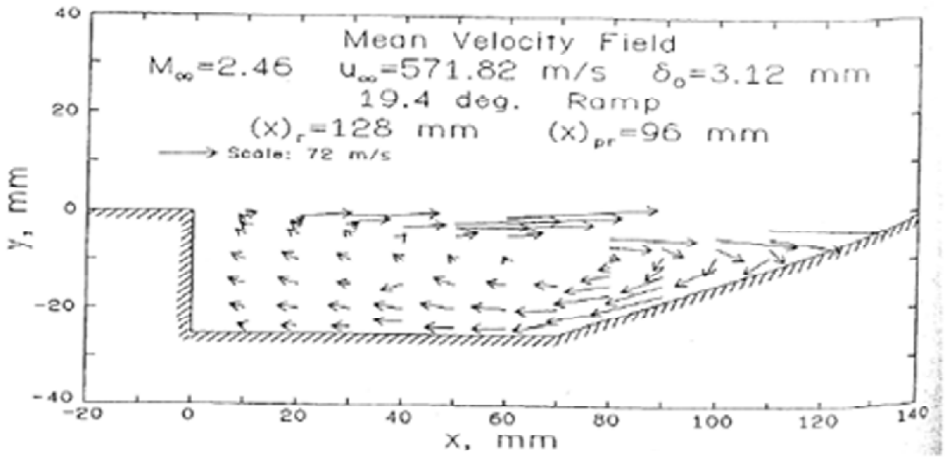

Figure 23: Velocity vector plot experimental

approximately in both the predicted results. In experiment too, the center of recirculation is found nearly in the same location. This recirculation of flow provides flame holding properties.

4.7. stream wise mean velocity profiles

The velocity profile at different sections perpendicular to the inlet is plotted for both the cases and shown in (Fig. 24 and Fig. 25). It clearly indicates the free shear layer over the cavity. It is compared with the experimental velocity profile (Fig. 26) and agreeing very well qualitatively.

4.8. Wall static pressure

The wall static pressure contour is plotted for both the cases (Fig. 27) the predicted results are in general grid independent. In the paper, it is clearly mentioned that the accuracy of the pressure measurements is approximately $\pm$ 0.6%. But the difference between predicted and experimental values for wall pressure is more than 0.6%. So, it seems that there are some other reason for this difference. As we know that the cavity flow is unsteady by nature which is tried to solve here as steady flow by slanting the rear wall of the cavity, but actually the flow may not be steady in the slant cavity too. This may be the reason for the difference in the wall static pressure.

4.9. Boundary layer redeveloping

In the experimental result, it was mentioned that there are free shear layer over the cavity followed by recompression of flow over the slanted wall up to a certain distance and then boundary layer in redeveloped at the end of slanted wall. To check the boundary layer redevelopment on the slanted wall, the velocity profile at different sections of the slanted wall perpendicular to the slanted wall itself is plotted for both the grids. It is observed that there is recirculation of flow in the beginning of slant wall and boundary layer is

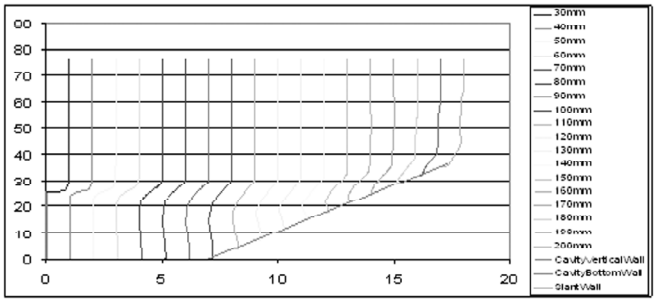

Figure 24: Stream wise mean velocity profile for grid-1

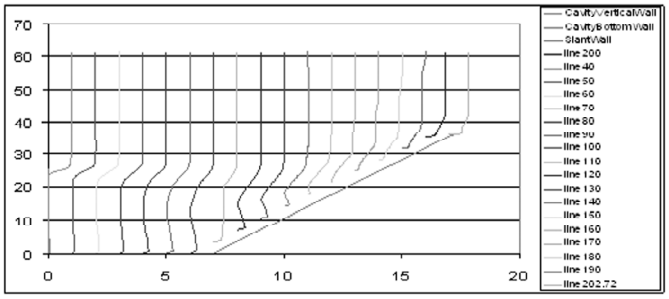

Figure 25: Stream wise mean velocity profile for grid-2

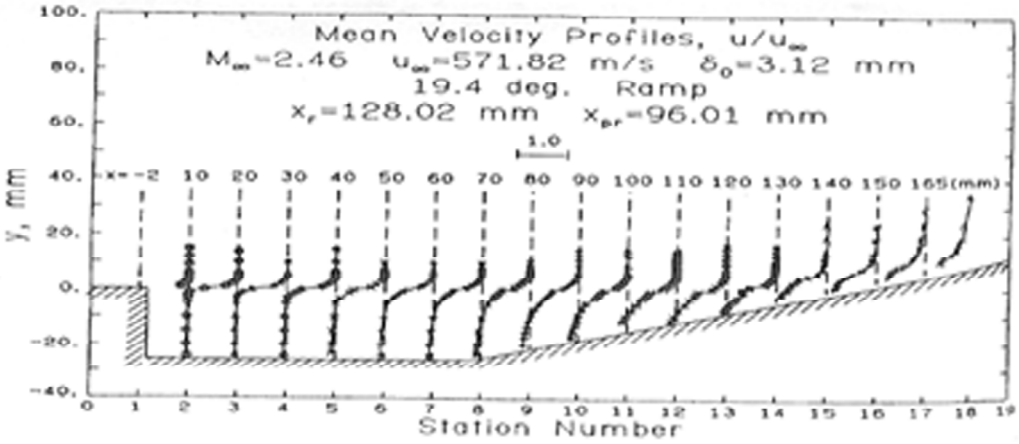

Figure 26: Stream wise mean velocity profile for Experimental

redeveloped at the end of slant wall. So, the boundary layer redevelopment is captured and qualitatively matching with the experiment.

4.10. Grid Independence Study

Two different grid size have been simulated for the same computational domain with the same boundary conditions. It is shown above that the predicted results for both the cases are close to each other. So, these solutions are considered as grid independent.

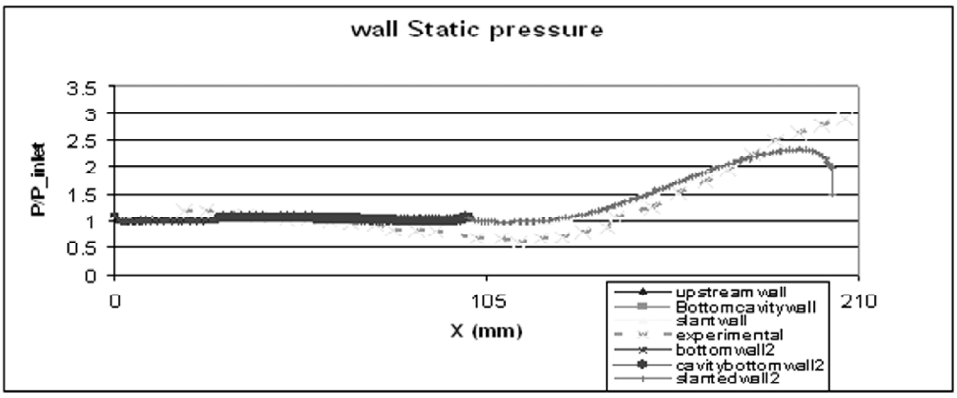

Figure 27: wall static pressure

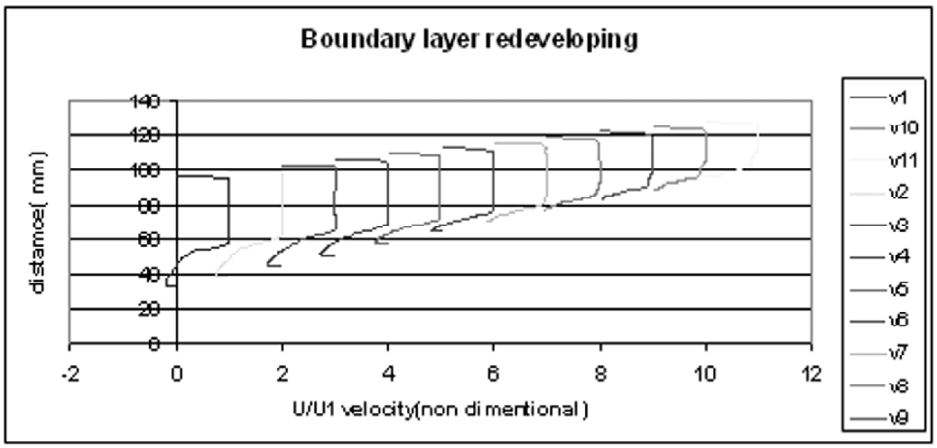

Figure 28: Boundary layer redeveloping for grid-1

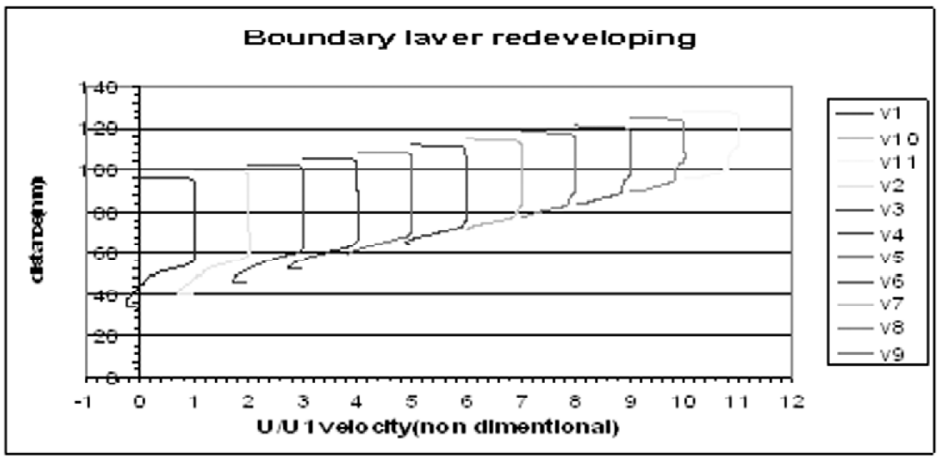

Figure 29: Boundary layer redeveloping for grid-2

5. CONCLUSIONS

1. Overall flow features like recirculation zone inside the cavity, free shear layer over the cavity, recompression zone on the slant wall, boundary layer redevelopment at the end of slant wall and oblique shock are qualitatively well predicted.
2. Sonic line (M = 1) is qualitatively agreeing well.
3. There is very good qualitative agreement in velocity profile at different section.
4. There is considerable difference in the predicted and measured wall static pressure all along the cavity and slant wall. The reason for the difference may be the unsteady nature of flow.
5. The predicted results are in general grid independent.

REFERENCES

[1] M. Samimy, H. L. Petrie. A study of compressible turbulent reattaching free shear layers. AIAA, Journal 24(2), 261-267, 1986.

[2] Anderson, J.D. Jr. *Computational fluid dynamics*, McGraw-Hill, Inc.1995.

[3] FLUENT 6, *User's Guide Volumes*, Fluent Incorporated.

[4] Patankar, S. V. *Numerical Heat transfer and Fluid Flow*, Hemisphere Publishers, Washington, D. C, 1980.

[5] Unaune, S.V. and V. Ganesan (2004) Flow field studies in an afterburner. *IE (I) Journal-MC*,84, 165-170.

[6] Versteeg, H. K and W. Malalasekera*An Introduction to Computational Fluid Dynamics-The Finite Volume Method*, Longman Group Ltd, 1995.

[7] Zhang, X. and H. Chiu (1987) Numerical Modeling of Afterburner Combustion. *International Journal of Turbo and Jet Engines*,4, 251-262.

[8] Ashfaque Ahmad Khan, Mixing enhancement in supersonic cavity flow. *A Thesis*, July 2007.

[9] A. Ben Yakar and Hanson R K. cavity flame holders for ignition and flame stabilization in scramjets: An overview. *Journal of propulsion and power*, 17(4): 869-877, 2001.

[10] R.C. Murray and G.S. Elliott. Characteristics of the compressible shear layer over a cavity. *AIAA Journal*, 39(5), May 2001.

[11] A.A. Khan and T. R. Shembharkar. Computation of high speed cold cavity flow with a commercial cfd code. *31st National conference on fluid mechanics and fluid power*, 1: 132-139, 16-18 December 2004.

[12] K.M. Kim, S.W. Baek and C.Y. Han. Numerical study on supersonic combustion with cavity-based fuel injection. Int*Journal of heat transfer and mass transfer*, 47:271-286, 2004.

[13] C.K. Kim, S.T.J. Yu, and Z.C. Zhang. Cavity flow in scramjet engine by space-time conservation and solution element method *AIAA Journal*, 42(5): 912-919, 2004.

[14] K.H. Yu, K.J. Wilson, and K.S. Schadow. Effect of flame-holding cavities on supersonic-combuction performance. *Journal of propulsion and power*,(17(6): 1287, 2001.

[15] D.L. Davis and R.D.W. Bowersox. computational fluid dynamics analysis of cavity flame holders for scramjets.*AIAA* 97-3270,1997.